RSC Advances

PAPER

View Article Online
View Journal | View Issue

Cite this: *RSC Adv.*, 2017, **7**, 55866

Integrated synthesis of metallocene@support catalysts based on glyphosate and its zirconium derivatives†

Annan Zhou,[a] Yuejuan Zhang,[b] Yasai Shi[a] and Qinghong Xu *[a]

Three new kinds of composite metallocene catalyst, Cp_2Zr@Gly, Cp_2Zr@ZrGp and Cp_2Zr@EXZrGP, for ethylene polymerization were synthesized based on matrixes of glyphosate (Gly), layered zirconium glyphosate (ZrGP) and exfoliated zirconium glyphosate (EXZrGP), and their catalytic activity in ethylene polymerization was studied. The catalytic activities of Cp_2Zr@Gly, Cp_2Zr@ZrGp and Cp_2Zr@EXZrGP are 3.8×10^5, 3.3×10^5 and 4.8×10^5 gPE per mol_{Zr} per h per bar at a temperature of 60 °C and after a time of 1.0 h, higher than that of the catalyst Cp_2ZrCl_2@SiO_2 (2.3×10^5 gPE per mol_{Zr} per h per bar), which is now used in industry. The catalytic activities of the three new catalysts are also higher than that of the catalyst Cp_2ZrCl_2 (3.0×10^5 gPE per mol_{Zr} per h per bar) under the same conditions. Exfoliation of the activity centers from the support and reactor fouling phenomena were all found to be avoided during the course of the polymerization.

Received 9th October 2017
Accepted 23rd November 2017

DOI: 10.1039/c7ra11089h

rsc.li/rsc-advances

1. Introduction

As an important material, polyolefin resin directly affects the development of a national economy and the level of national consumption is closely related to the developments of packaging, agriculture, construction, automobiles and electronics. Polyolefin products have been widely used in aerospace, aviation, electronics, national defence and other important areas and so have become a benchmark of modern economic development.[1,2]

Catalysts play an important role in the polyolefin industry. This includes the main catalyst, cocatalyst and support, and each part is interrelated and inseparable. Olefin polymerization catalysts have included Ziegler–Natta, metallocene and post-metallocene catalysts in the past few decades. Metallocene, a type of single active center catalyst, is one kind of important catalyst for olefin polymerization after the Ziegler and Ziegler–Natta catalysts, which was found by Natta and Breslow in 1957.[3–5] Compared to a Ziegler–Natta catalyst, metallocene has unique catalytic characteristics and is superior. Firstly, due to its single active center, the polymers produced have high structural homogeneity and narrow molecular weight distribution. Secondly, polymers produced with different structural catalysts have multiple properties, and this will extend the applications of the polymers. Thirdly, this catalyst has wide monomer adaptability and stereoselectivity in polymerizations.

Although metallocene has advantages in olefin polymerizations, reactor fouling in the gas-phase and slurry-phase processes often happened, which brought many troubles and safety concerns to polyolefin industrial productions. In addition, the large amount of cocatalyst (mainly MAO) used to achieve high catalytic efficiency increases the production cost accordingly at the same time. Thus, the catalyst needs to be supported on a carrier with high stability. The immobilization not only can improve the polymer's morphology, increase the apparent density and control the particle size distribution of the polymer, but also decreases the inactivation of the molecular association between two loaded active centers, and the amount of the cocatalyst used (such as the ratio of aluminum and zirconium) can also be greatly reduced. Additionally, the β-H elimination reaction in polymerization can be decreased greatly at the same time and a polymer with high molecular weight, high melting point, high stereoregularity and aging resistance can be obtained.

In the past few decades, many different kinds of support (*e.g.*, $MgCl_2$, SiO_2, zeolite, montmorillonite, α-ZrP and polystyrene) and immobilization procedure have been investigated.[6–14] The most commonly used carriers are spherical $MgCl_2$ and silica gel. $MgCl_2$ is often used for Ziegler–Natta catalysts and silica gel is often used for metallocenes. However, spherical $MgCl_2$ is brittle and easily damaged, which results in unstable performance of the catalysts and exfoliation of the catalyst from the surface of the carriers often happens. A similar phenomenon of exfoliation of the catalyst also happens to the spherical silica gel. An effective way to solve the above problems is to realize an integrated synthesis

[a]*State Key Laboratory of Chemical Resource Engineering, Beijing University of Chemical Technology, Box. 98, 15 Beisanhuan Donglu, Beijing 100029, P. R. China. E-mail: xuqh@mail.buct.edu.cn*

[b]*Beijing Vocational College of Agriculture, No. 46, Beiyuan Road, Chaoyang District, Beijing 100012, P. R. China*

† Electronic supplementary information (ESI) available. See DOI: 10.1039/c7ra11089h

between the catalyst and carrier under the conditions of the active, unreduced catalyst. There are two methods to achieve the above target. One is to connect the active center to the framework of the carrier during the synthesis of the carrier, and another is the modification and synthesis of the catalyst on the surface of the carrier. For the second way, the coverage of the catalyst on the surface of the carrier must be maximized.

Since the 1970s, phosphonate compounds, including zirconium phosphonates,[15] aluminum phosphonates,[16] titanium phosphonates,[17] *etc.*, have been synthesized. High heat resistance, crush resistance, a certain degree of flexibility and coordinative properties endow the materials a wide range of applications. Glyphosate zirconium (ZrGp), a type of layered organic/inorganic composite material with coordinative groups in its framework, was synthesized successfully in 2010, and the material was widely studied in coordinations,[18] preparation of super hydrophobic materials[19] and adsorptions.[20] In this paper, two kinds of new composite catalyst, Cp_2Zr@ZrGp and Cp_2Zr@EXZrGP, were successfully synthesized by grafting Cp_2Zr onto a framework of ZrGp and exfoliated glyphosate zirconium (EXZrGP). Additionally, a new composite catalyst, Cp_2Zr@Gly, was also synthesized by grafting Cp_2Zr onto a chemical chain of glyphosate (Gly). Catalytic activities of the three composite catalysts in ethylene polymerization were studied. The results indicate that the activities of these three catalysts are higher than those of the composite catalyst Cp_2ZrCl_2@SiO_2 (Cp_2ZrCl_2 was supported on spherical SiO_2, a type of catalyst commonly used in industry) and the homogeneous catalyst Cp_2ZrCl_2, and the activity of Cp_2-Zr@EXZrGP is higher than that of Cp_2Zr@ZrGp. The regents in this study are cheap enough and the synthetic method to obtain the catalysts is not complex. These composite catalysts are expected to have good application prospects in industry.

2. Experiment

2.1. Chemicals

All chemicals used are of analytical grade and were obtained from commercial suppliers. Zirconium dichloride oxide octahydrate ($ZrOCl_2 \cdot 8H_2O$, ≥99.0), hydrofluoric acid (HF), methylaluminoxane (MAO, 1.5 M solution in toluene), silica gel 2408d, bis(cyclopentadienyl)zirconium dichloride (≥98%, Cp_2ZrCl_2), zirconium tetrachloride (≥99.0%), ethylamine (≥99.0%), ethanol (≥99.5%), ethylenediamine (≥98.0%), xylene (≥99.0%), toluene (≥99.0%), magnesium strips, tetrahydrofuran (≥99.0%, THF), sodium (≥99.0%) and iodine (≥99.0%) were obtained from Beijing Chemical Reagent Company; glyphosate (≥95%) was obtained from Sinopharm Chemical Reagent Company; sodium cyclopentadiene (≥99.5) was obtained from J&K Chemical Company.

The absolute ethanol was obtained as follows: 5.0 g polished magnesium strips and 0.5 g iodine were mixed with 60 mL ethanol and the mixture was refluxed until the magnesium was completely consumed, then 900 mL ethanol was added. The solution was refluxed for 1 h and distilled. $ZrCl_4$ and glyphosate were dried in a vacuum oven at 120 °C for 6 h. The dried ethylamine, ethylenediamine, xylene, toluene and THF were obtained by adding some sodium, refluxing for 1 h and distilling.

2.2. Synthesis of Cp_2Zr@Gly

5.0 g (about 0.02 mol) of dried $ZrCl_4$ was added to 50 mL of glyphosate solution in absolute ethanol (the molar concentration of glyphosate in ethanol is about 0.43 M). After the mixture was stirred for 24 h at 70 °C under the protection of nitrogen gas, the product (named as $GlyZrCl_2$) was then obtained by vacuum filtration. 20 mL of absolute dried THF (used as a reagent) and 3.5 g sodium cyclopentadienylide were mixed with $GlyZrCl_2$ and the mixture was stirred for about 48 h at room temperature under the protection of nitrogen gas. The final product, Cp_2Zr@Gly (about 8.3 g, the yield of the product is about 70%), was obtained after the solvent was removed under low pressure, extracted in dichloromethane by Soxhlet for 48 h, recrystallized in xylene for 12 h and then dried in a vacuum environment. The elemental composition of Cp_2Zr@Gly was analyzed and is listed in Table 1. Solid-state ^1H MAS NMR (δ): 2.0 (PO_3H_2, 2H, t); 2.0 (NH, 1H, m); 2.6 (α-H to –N–C, methylene, 2H, t); 2.9 (α-H, cyclopentadiene, 2H, t); 3.5 (α-H to –C(=O)O, methylene, 2H, t); 6.4 (β-H, cyclopentadiene, 4H, t); 6.5 (γ-H, cyclopentadiene, 4H, t); 11.0 (COOH, 1H, t). Solid-state ^{31}P MAS NMR (δ): 15.39 (PO_3H_2), which is shown in Fig. S1.†

2.3. Synthesis of Cp_2Zr@ZrGp

ZrGp was synthesized according to the method in ref. 18. Under the protection of nitrogen gas, 2.0 g of dried $ZrCl_4$ was added into a mixture of ZrGp (5.0 g) in absolute ethanol (50 mL). After the mixture was stirred at 70 °C for 24 h, it was transferred and sealed in an autoclave (filled by nitrogen gas), and kept at 80 °C for 30 days. After the mixture was then filtered using a vacuum pump to remove the ethanol and the solid was degassed 2–3 times in liquid nitrogen, 30 mL of THF and 1.0 g of sodium cyclopentadienylide were added to the above degassed solid, and the mixture was stirred for about 48 h at room temperature under the protection of nitrogen gas. The final product, Cp_2-Zr@ZrGP (about 6.7 g), was obtained after the solvent was removed under low pressure, extracted in dichloromethane by Soxhlet for 48 h, recrystallized in xylene for 12 h and then dried in a vacuum environment. The elemental composition of Cp_2-Zr@ZrGP was analyzed and is listed in Table 1.

2.4. Exfoliation of ZrGp and synthesis of Cp_2Zr@EXZrGP[21]

5 g of ZrGp was immersed in 30 mL of ethylamine. After the mixture was refluxed for 1 hour and vibrated in an ultrasonic oscillator for 10 minutes, the layered material was exfoliated.

Table 1 Elemental analysis (%) in $GlyZrCl_2$, Cp_2Zr@Gly, ZrGP, $ZrGPZrCl_2$, Cp_2Zr@ZrGp, EXZrGP and Cp_2Zr@EXZrGP

	C (%)	H (%)	O (%)	N (%)	P (%)	Zr (%)	Cl (%)
$GlyZrCl_2$	17.87	3.97	39.72	6.95	15.39	9.04	7.05
Cp_2Zr@Gly	28.11	4.68	37.50	6.53	14.52	8.53	0.13
ZrGP	15.98	3.00	40.81	6.29	13.91	20.00	0.00
$ZrGPZrCl_2$	14.41	2.80	38.44	5.60	12.41	22.77	3.55
Cp_2Zr@ZrGp	19.35	3.18	37.54	5.48	12.13	22.21	0.11
EXZrGP	15.95	3.04	40.78	6.25	13.93	19.98	0.00
Cp_2Zr@EXZrGP	23.18	3.33	33.71	4.92	10.88	23.91	0.07

The solid exfoliated ZrGp was protected under nitrogen gas after it was filtered, washed with dried toluene and dried in a vacuum environment.

Under the protection of nitrogen gas, 1.0 g of the ZrGp exfoliated by ethylamine and 1.0 g of $ZrCl_4$ were added into 30 mL of dehydrated and degassed toluene, and the mixture was refluxed for about 24 h. The above mixture was transferred to and sealed in an autoclave (filled by nitrogen gas), and kept at 80 °C for 30 days. The mixture was then filtered using a vacuum pump to remove the solvent and the solid was degassed several times in liquid nitrogen. 30 mL of THF and 1.0 g of sodium cyclopentadienylide were added to the above degassed solid, and the mixture was stirred for about 48 h at room temperature under the protection of nitrogen gas. The final product, Cp_2Zr@EXZrGP (about 2.2 g), was obtained after the solvent was removed under low pressure, extracted in dichloromethane by Soxhlet for 48 h, recrystallized in xylene for 12 h and then dried in a vacuum environment. The elemental composition of Cp_2Zr@EXZrGP was analyzed and is listed in Table 1.

2.5. Synthesis of Cp_2ZrCl_2@SiO_2

Silica (5 g) and MAO (25 mL, 1.5 mol L^{-1} in dry toluene) were stirred together for 1 h at 30 °C, and a solution of Cp_2ZrCl_2 (50 mg of Cp_2ZrCl_2, 1 mL of MAO in 16 mL of dry toluene) was added. The mixture was stirred for 1 h at 40 °C, extracted in dichloromethane by Soxhlet for 48 h, recrystallized in xylene for 12 h and then dried under vacuum for 4 h (0.3 kPa, 25 °C). The composite catalyst was obtained. All the steps above were finished under the protection of nitrogen gas.

FT-IR analysis and diffusion reflectance UV-vis (DR UV-vis) analysis of the composite catalyst are shown in Fig. S2 and S3 in the ESI.†

The syntheses, including of Cp_2Zr@Gly, Cp_2Zr@ZrGp, Cp_2Zr@EXZrGP and Cp_2ZrCl_2@SiO_2, were carried out in Schlenk-tubes on a vacuum line, and all of the processes in the reactions were protected by nitrogen gas and the product was also protected in an environment of nitrogen gas.

2.6. Polymerization procedure

100 mg of the catalyst, 2.0 mL of 2.4 M triethylaluminium (TEAL, in dried hexane) and 1.0 L of dried hexane were added to a high-pressure ampule (2.0 L). Ethylene gas was continuously fed into the ampule at 1.0×10^6 Pa during polymerization at 60 °C. One hour later, the reaction was stopped. The polymer was quickly filtered and dried in a vacuum oven at 60 °C for 12 h.

2.7. Sample characterizations

The DR UV-vis absorptions of the samples were obtained with a Shimadzu UV-3600 ultraviolet and visible spectrophotometer (made in Japan). Fourier transform infrared (FT-IR) spectra were recorded in the range of 4000–400 cm^{-1} with a 2 cm^{-1} resolution on a Bruker Vector-22 Fourier transform spectrometer (made in Germany) using the KBr pellet technique (1.0 mg of sample in 100.0 mg of KBr). X-ray photoelectron spectroscopic (XPS) analysis was performed on Shimadzu ESCA-750 and ESCA-1000 spectrometers (made in Japan) with Mg K_α X-ray sources. Solid-state ^{13}C MAS NMR spectra of the samples were obtained with a Bruker AV600 (made in Germany). Crystal structures of the products were examined using a Rigaku D/MAX powder X-ray diffractometer (PXRD) (made in Japan) with a Cu K_α X-ray source ($\lambda = 0.15406$ nm, scanning speed is 10° min^{-1}). Scanning electronic microscopy (SEM) images of the products were observed on a Shimadzu SS-550 microscope (made in Japan) at 15 keV. The chemical compositions of Zr and P were determined by inductively coupled plasma (ICP) with a Perkin-Elmer plasma 40 emission spectrometer (made in Japan) and C, O, N, Cl and H were analyzed on a Vario-EL elemental analyzer (made in Germany). The M_w values and polydispersities (M_w/M_n) of the polymers were measured at 140 °C on a PlomerChar GPC-IR (made in Spain), using 1,2,4-trichlorobenzene as the solvent, and the columns were calibrated with narrow M_w polystyrene standards.

The samples prepared for DR UV-vis spectrometry, FT-IR spectrometry and solid-state ^{13}C MAS NMR spectrometry were all kept in a glove box filled with nitrogen gas.

3. Results and discussion

3.1. Synthesis and characterizations of the supported catalysts

The new catalysts were synthesized based on the existence of amino and carboxyl groups in frameworks of Gly, ZrGp and exfoliated ZrGp. Firstly, in the molecular structure of Gly, the

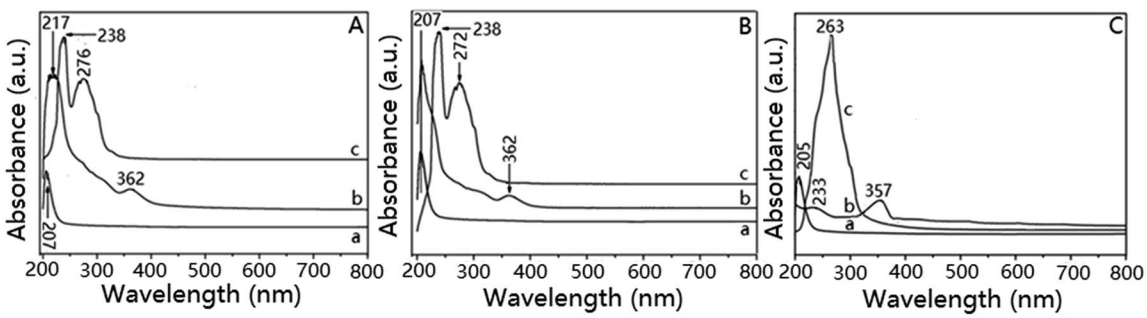

Fig. 1 UV-vis spectra of (A): Gly (a), $GlyZrCl_2$ (b) and Cp_2Zr@Gly (c); (B): ZrGP (a), $ZrGPZrCl_2$ (b) and Cp_2Zr@ZrGp (c); (C): EXZrGP (a), $EXZrGPZrCl_2$ (b) and Cp_2Zr@EXZrGP (c).

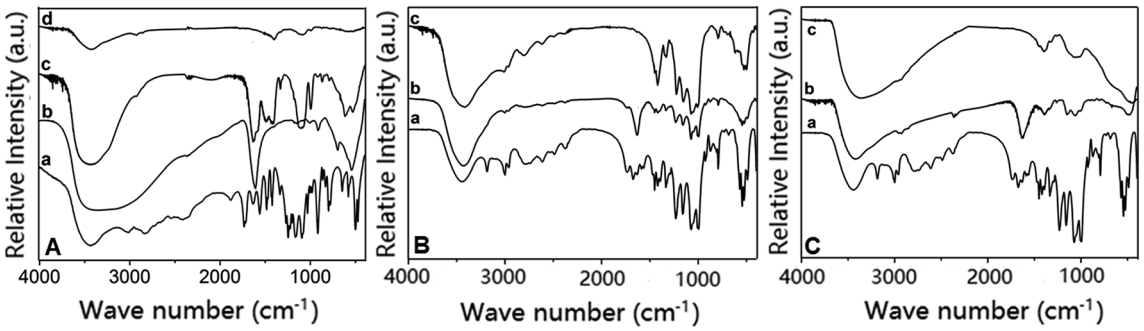

Fig. 2 FT-IR spectra of (A): Gly (a), $ZrCl_4$ (b), $GlyZrCl_2$ (c) and Cp_2Zr@Gly (d); (B): ZrGP (a), $ZrGPZrCl_2$ (b) and Cp_2Zr@ZrGp (c); (C): EXZrGP (a), $EXZrGPZrCl_2$ (b) and Cp_2Zr@EXZrGP (c).

amino and carboxyl groups coordinated with $ZrCl_4$ to form a stable five ring structure after two Cl atoms in the $ZrCl_4$ were removed. The composite catalyst Cp_2Zr@Gly was finally formed after the reaction between $GlyZrCl_2$ and sodium cyclopentadienylide. Secondly, the distance between the layers of ZrGp is about 1.65 nm, which permits the entrance of $ZrCl_4$. After the $ZrCl_4$ molecules entered into the layers of ZrGp, they coordinated with the amino and carboxyl groups and connected to the wall of ZrGp to form $ZrGPZrCl_2$. The new composite catalyst Cp_2Zr@ZrGp was formed after the molecules of sodium cyclopentadienylide were driven into the layers of $ZrGPZrCl_2$. Thirdly, in order to eliminate blocking of the narrow gap of ZrGP, the layered compound was exfoliated by ethylamine to allow the amino and carbonyl groups to enter. Molecules of $ZrCl_4$ reacted with the above two groups to form $EXZrGPZrCl_2$, and the composite catalyst Cp_2Zr@EXZrGP was finally synthesized by the reaction between $EXZrGPZrCl_2$ and sodium cyclopentadienylide.

The DR UV-vis absorption spectra of the composite catalysts and some intermediate products are shown in Fig. 1. The absorption at 207 nm, attributed to Gly, was found to be moved to 217 nm in the spectrum of $GlyZrCl_2$ (Fig. 1A(b)), and a weak absorption at 362 nm appeared in the spectrum of $GlyZrCl_2$ at the same time. These changes possibly came from redistribution of the internal electronic cloud in Gly during the formation of $GlyZrCl_2$. In addition, the appearance of a strong absorption at about 276 nm, attributed to C=C[15] in Cp_2Zr@Gly (Fig. 1A(c)), confirms the coordination between the CP rings and Zr atoms. Similar to Cp_2Zr@Gly, the DR UV-vis absorptions of ZrGP (Fig. 1B(a)) also have a small shift from 200 to 207 nm for $ZrGPZrCl_2$ (Fig. 1B(b)), and a weak absorption at 362 nm appears for $ZrGPZrCl_2$ at the same time. The absorption of C=C in cyclopentadienyl for Cp_2Zr@ZrGp (Fig. 1B(c)) is found at 272 nm, proving the existence of $ZrCP_2$ in the framework of ZrGP. The DR UV-vis absorption of $EXZrGPZrCl_2$ at about 205 nm had a large shift (from 205 to 263 nm, Fig. 1C(b)), and the absorption of C=C for cyclopentadienyl in Cp_2Zr@EXZrGP is found at 263 nm.

The above results were also proven by FT-IR spectrometry (Fig. 2). Infrared absorptions (720, 1000 and 1410 cm^{-1} for Cp_2Zr@Gly; 720, 1000 and 1410 nm for Cp_2Zr@ZrGp and 720, 980 and 1410 cm^{-1} for Cp_2Zr@EXZrGP) from the

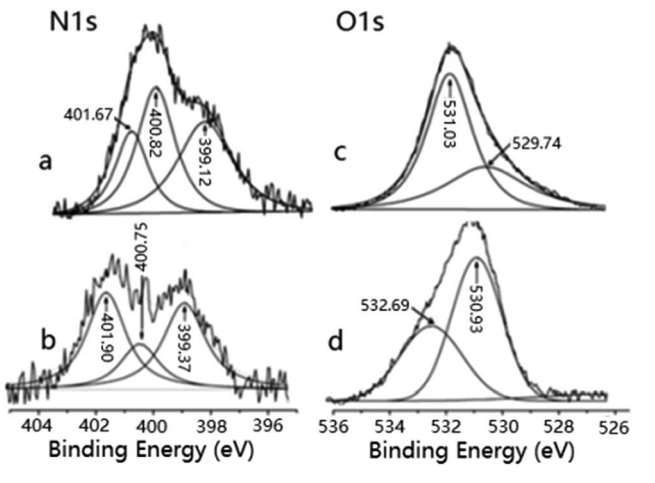

Fig. 3 XPS spectra of N 1s and O 1s for Gly (a and c) and $GlyZrCl_2$ (b and d).

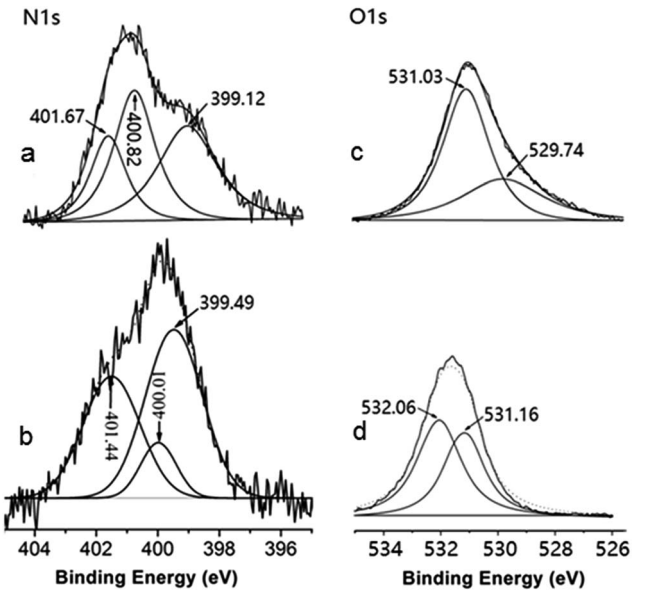

Fig. 4 XPS spectra of N 1s and O 1s for ZrGP (a and c) and $ZrGPZrCl_2$ (b and d).

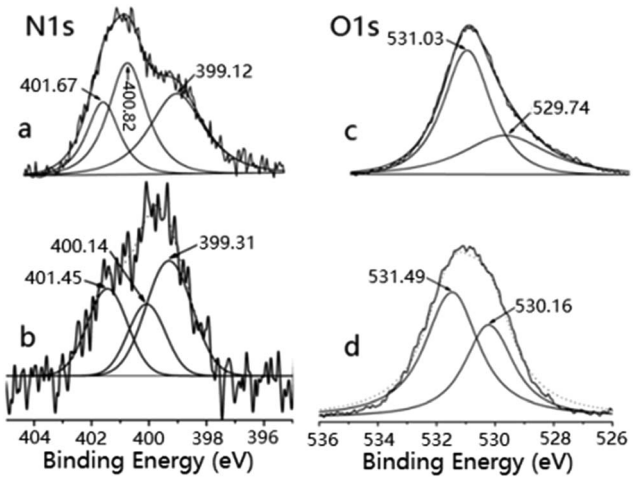

Fig. 5 XPS spectra of N 1s and O 1s for EXZrGP (a and c) and EXZrGPZrCl$_2$ (b and d).

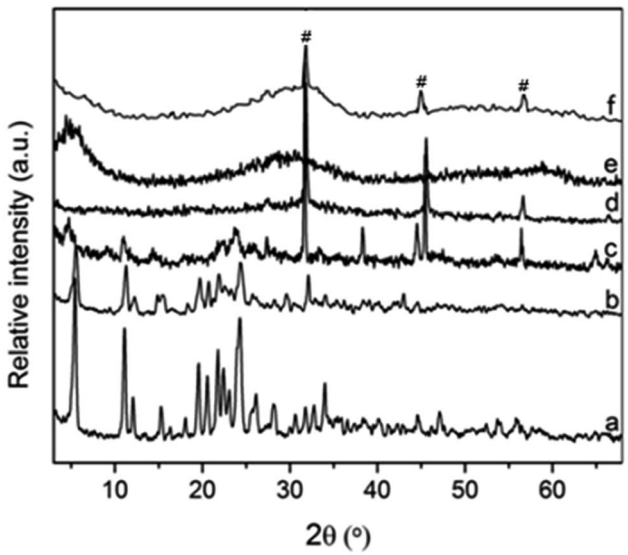

Fig. 7 XRD patterns of ZrGP (a), ZrGPZrCl$_2$ (b), Cp$_2$Zr@ZrGp (c), Cp$_2$Zr@Gly (d), EXZrGP (e) and Cp$_2$Zr@EXZrGP (f).

cyclopentadiene ring[22] are all found in the spectra of the composite catalysts. Also, the absorptions coming from Zr–O (at about 1108 cm^{-1}) and C–H (at about 2981 cm^{-1}) are found in the corresponding spectra of the catalysts. Although the samples prepared for the measurements were all kept in a glove box filled with nitrogen gas, they still adsorbed some water molecules during the characterizations and so a peak at about 1610–1630 cm^{-1} from water absorption was found in the figure. A broad band from 3300 cm^{-1} to 3600 cm^{-1} comes from the uncoordinated hydroxyl groups and adsorbed water.

The XPS spectra of N 1s and O 1s for the intermediate products and the catalysts are shown in Fig. 3–5. Compared to the binding energies (BEs) of N 1s and O 1s in Gly (Fig. 3a and c), it is clearly observed that the BEs of N_{N-H}, N_{N-C} and N_{N-COOH} in GlyZrCl$_2$ (Fig. 3b) are much-changed, while the BEs of $O_{O=C}$ and O_{O-H} have similar results (Fig. 3d). The BEs of N_{N-H} and N_{N-COOH} increase by 0.25 eV (from 399.12 to 399.37 eV) and 0.23 eV (from 401.67 to 401.90 eV), respectively; while the BE of N_{N-C} decreases by 0.07 eV (from 400.82 to 400.75 eV); the BEs of $O_{O=C}$ and O_{O-H} increase by 1.63 eV (from 531.03 to 532.69 eV) and 1.19 eV (from 529.74 to 530.93 eV), respectively.

Big changes in the binding energies (BEs) of N 1s and O 1s in N–H, N–C, N–COOH, O=C and O–H are found for ZrGPZrCl$_2$ (Fig. 4b and d) compared to those for ZrGP (Fig. 4a and c). Compared to that of ZrGP, the BE of N 1s in N–H increases by 0.37 eV (from 399.12 to 399.49 eV), however it decreases by 0.81 eV (from 400.82 to 400.01 eV) and 0.23 eV (from 401.67 to 401.44 eV) in N–C and N–COOH; the BEs of O 1s increase by 1.03 eV (from 531.03 to 532.06 eV) and 1.42 eV (from 529.74 to 531.16 eV). The changes in the BEs of the relative elements prove the existence of coordination between ZrGP and Zr (in the ZrCl$_2$ group).

Compared to that of EXZrGP (Fig. 5a), the BE of N_{N-H} for EXZrGPZrCl$_2$ (Fig. 5b) increases by 0.19 eV (from 399.12 to 399.31 eV), and the BEs of N_{N-C} and N_{N-COOH} decrease by 0.68 eV (from 400.82 to 400.14 eV) and 0.22 eV (from 401.67 to 401.45 eV), respectively. The BEs of $O_{O=C}$ and O_{O-H} for EXZrGPZrCl$_2$ (Fig. 5d) increase by 0.46 eV (from 531.03 to 531.49 eV) and 0.42 eV (from 529.74 to 530.16 eV) compared to those in the corresponding data for EXZrGP (Fig. 5c), respectively.

The coordination effect results in changes to the electron densities outside the nucleus of the nitrogen and oxygen atoms in the intermediate products.

Solid-state ^{13}C MAS NMR spectra of Gly, Cp$_2$Zr@Gly, Cp$_2$Zr@ZrGp and Cp$_2$Zr@EXZrGP are shown in Fig. 6. These spectra indicate that the $\delta_{C=C}$ values in the CP ring[23] in Cp$_2$Zr@Gly (Fig. 6A(b)), Cp$_2$Zr@ZrGp (Fig. 6B) and Cp$_2$Zr@EXZrGP

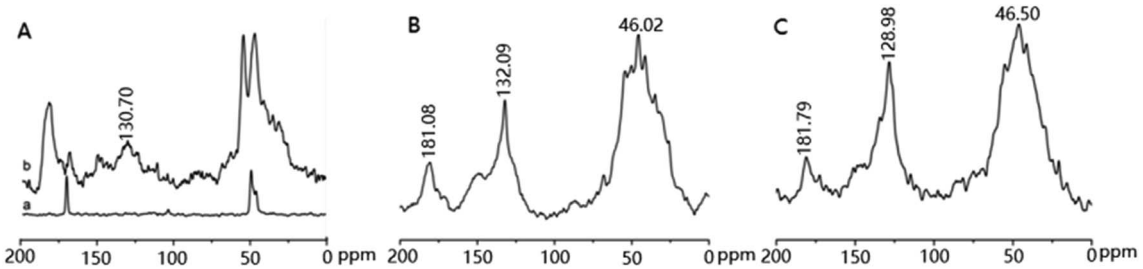

Fig. 6 ^{13}C NMR spectra of Gly (A(a)), Cp$_2$Zr@Gly (A(b)), Cp$_2$Zr@ZrGp (B) and Cp$_2$Zr@EXZrGP (C).

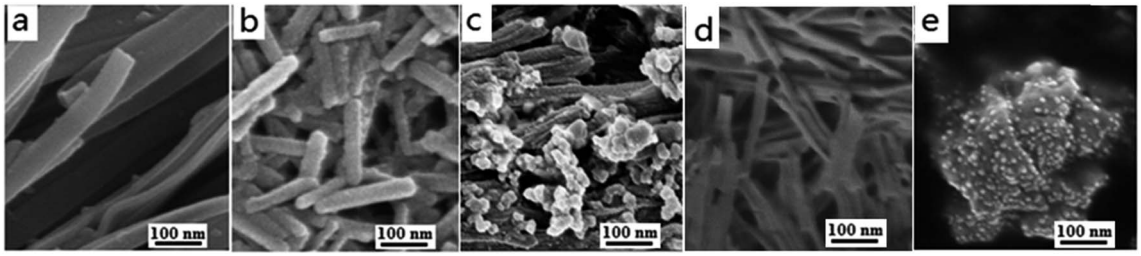

Fig. 8 SEM images of ZrGP (a), EXZrGP (b), Cp_2Zr@ZrGp (c), Cp_2Zr@EXZrGP (d) and Cp_2Zr@Gly (e).

(Fig. 6C) are at about 130.70 ppm, 132.09 ppm and 128.98 ppm, respectively, however, this peak doesn't exist in the spectrum of Gly. Also $\delta_{C=O}$ and δ_{C-H}, attributed to the uncoordinated carboxyl groups and the organic chain, are also found at about 181.00 ppm and 46.00 ppm.

Three main peaks (at 31.73°, 45.64° and 56.63°, marked with #) attributed to diffractions of metallocene[24] are found in the PXRD patterns of Cp_2Zr@Gly (Fig. 7d), indicating the formation of a Cp_2Zr structure on the chemical chain. The diffraction at 5.04° in ZrGP was found to be shifted to 4.72° after $ZrCP_2$ formed and connected to the layered framework (Fig. 7c). The interlayer space of ZrGP increased by about 2.4 Å, similar to the height of $ZrCp_2$.[25] The characteristic diffractions (at 31.67°, 45.50° and 56.51°) representing the metallocene structure in the spectrum prove the formation of $ZrCp_2$ in the inner layers. Additionally, the intensities of most of the diffractions of Cp_2Zr@ZrGp are weaker than those of ZrGP, indicating that the crystallinity of ZrGP was reduced after the $ZrCp_2$ structure formed.

As to the formation of Cp_2Zr@EXZrGP, ZrGp was firstly exfoliated using ethylamine as the exfoliating reagent. The PXRD pattern (Fig. 7e) indicates that all of the characteristic diffractions of ZrGp disappeared and two wide diffraction areas appeared around 5° and 30° after the layered material was exfoliated, indicating that the regular layered structure was destroyed.[26] Also it is found that the layered structure was not recovered during the formation of Cp_2Zr@EXZrGP, but the diffractions from the metallocene structure (marked with # on the top in the figure) are found (Fig. 7f), proving the formation of the $ZrCP_2$ structure in the catalyst.

SEM images of ZrGP, EXZrGP, Cp_2Zr@ZrGp, Cp_2Zr@EXZrGP and Cp_2Zr@Gly are shown in Fig. 8. The catalyst Cp_2Zr@Gly has a cluster shape morphology (Fig. 8e), and an amount of small particles are evenly distributed on the surface of the clusters. The small particles possibly come from a zirconocene structure. H-bond interactions in the material are the main reason for the formation of this morphology. In ZrGP a long regular bamboo sheet morphology is observed (shown in Fig. 8a), but the basic morphology was not damaged during the course of the formation of Cp_2Zr@ZrGp. Many small particles are found to exist on the cross section and few on the outer surface of the layers, showing that most $ZrCp_2$ groups locate in the layers. After ZrGP was exfoliated, the regular strip shape was shortened greatly and a breaking effect happened during the exfoliation (Fig. 8b). Little change is found in the morphologies between Cp_2Zr@EXZrGP (Fig. 8d) and EXZrGP, and a few small

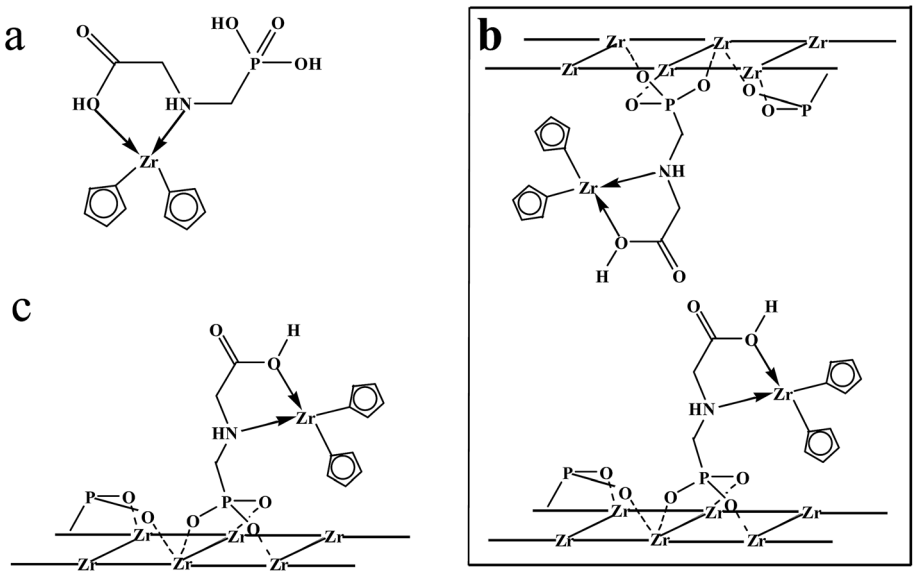

Fig. 9 Basic framework of Cp_2Zr@Gly (a), Cp_2Zr@ZrGp (b) and Cp_2Zr@EXZrGP (c).

Table 2 Zr content, ethylene polymerization activities, molecular weights (M_w) and polydispersities (M_w/M_n) of various catalysts

	Zr content (%)	Activity (gPE per mol_{Zr} per h per bar)	M_w	M_w/M_n
Cp_2ZrCl_2	31.2	3.0×10^5	1.7×10^5	2.81
Cp_2Zr@Gly	8.53	3.8×10^5	2.7×10^5	2.78
Cp_2ZrCl_2@SiO_2	0.2	2.3×10^5	2.5×10^5	3.22
Cp_2Zr@ZrGp	4.40 (in $ZrCp_2$)	3.3×10^5	2.1×10^5	2.33
Cp_2Zr@EXZrGP	7.98 (in $ZrCp_2$)	4.8×10^5	2.3×10^5	2.29

Table 3 Catalytic activities (gPE per mol_{Zr} per h per bar) of Cp_2Zr@Gly, Cp_2Zr@ZrGp and Cp_2Zr@EXZrGP at different temperatures in ethylene polymerization (the system pressure is 1.0×10^6 Pa)

Polymerization temperature (°C)	Cp_2Zr@Gly	Cp_2Zr@ZrGp	Cp_2Zr@EXZrGP
40	2.9×10^5	3.1×10^5	3.5×10^5
60	3.8×10^5	3.3×10^5	4.8×10^5
80	4.4×10^5	3.4×10^5	4.9×10^5

nanoparticles are found on the exfoliated ZrGP, due to the uniform distribution of the $ZrCP_2$ structure on the exfoliated strips.

Elemental analysis (%) in $GlyZrCl_2$, Cp_2Zr@Gly, ZrGP, $ZrGPZrCl_2$, Cp_2Zr@ZrGp, EXZrGP and Cp_2Zr@EXZrGP was performed with a Shimadzu ICPS-75000 inductively coupled plasma emission spectrometer (ICP-ES), and the percentages of N, H, O, P, Cl, C and Zr in the samples are listed in Table 1. Calculations show that the chemical compositions of Cp_2Zr@Gly and $ZrGPZrCp_2$ are $C_3H_8NO_5P{\cdot}Zr_{0.2}(C_{10}H_{10})_{0.2}$ and $C_6H_{14}N_2O_{12}P_2Zr{\cdot}Zr_{0.25}(C_{10}H_{10})_{0.25}$, respectively. Schemes illustrating the structures of the catalysts are shown in Fig. 9.

3.2. Catalytic activities of Cp_2Zr@Gly, Cp_2Zr@ZrGp and Cp_2Zr@EXZrGP in ethylene polymerizations

Cp_2Zr@Gly, Cp_2Zr@ZrGp and Cp_2Zr@EXZrGP have been tested for their performance in the slurry-phase polymerization of ethylene in hexanes in the presence of TEAL as the cocatalyst. The polymerization reactions proceeded very smoothly, producing free-flowing polyethylene in high yields. No evident reactor fouling was found except for with Cp_2Zr@Gly. With a temperature and time of 60 °C and 1.0 h, the catalytic activities of Cp_2Zr@Gly, Cp_2Zr@ZrGp and Cp_2Zr@EXZrGP are 3.8×10^5, 3.3×10^5 and 4.8×10^5 gPE per mol_{Zr} per h per bar, respectively. The activity sequence is possibly relative to the content of $ZrCp_2$ in the catalysts. Due to no elemental Cl being found, and 8.53% content of Zr in Cp_2Zr@Gly, the Zr atoms from $ZrCl_4$ that connected to Gly are considered to all come from the $ZrCp_2$ groups in the catalyst. Calculations show that about 1.0 mol Gly can form 0.2 mol of $GlyZrCp_2$. Considering that the amounts of Zr in ZrGP and Cp_2Zr@ZrGp are about 17.81% and 22.21%, respectively, the Zr content in $ZrCp_2$ is about 4.40%, lower than that of Cp_2Zr@Gly. As for EXZrGP, the space obstacle in the formation of Cp_2Zr connected to the wall of ZrGP was completely eliminated. $ZrCl_4$ could freely coordinate with the amino and carboxyl groups on the surface of the exposed single layer and Cp_2Zr could be formed easily. The mass content of $ZrCp_2$ (the Zr content in $ZrCp_2$ in Cp_2Zr@EXZrGP is about 7.98%) in Cp_2Zr@EXZrGP is about 19.40%, which is more than that in Cp_2Zr@ZrGp (10.81%) and less than that in Cp_2Zr@Gly (20.73%). Based on the mass content of $ZrCp_2$ in the catalysts and the activities of these catalysts, the catalytic activity of Cp_2Zr@EXZrGP is 1.26 and 1.45 times that of Cp_2Zr@Gly and Cp_2Zr@ZrGp, respectively.

The catalytic activities of the newly synthesized catalysts in ethylene polymerization were compared to those of the catalysts Cp_2ZrCl_2 and Cp_2ZrCl_2@SiO_2 (a type of heterogeneous catalyst used in industry at present), which were checked under the same conditions. It is found that the activities of the three catalysts are all higher than those of Cp_2ZrCl_2 and Cp_2ZrCl_2@SiO_2. The content of Zr in the related catalysts and their activities in ethylene polymerization are listed in Table 2.

The dependence of the catalytic activities of the above three catalysts on times and temperatures in ethylene polymerization was studied, and some data are listed in Tables 3 and 4. Considering the safety of the experiment and possible industrial applications in the future, the top-temperature in this study was controlled at 80 °C as large amounts of the solvent *n*-hexane would be volatilized and the pressure in the autoclave would be increased greatly. The catalytic activity of all three catalysts was found to increase with the increase in

Table 4 Catalytic activities (gPE per mol_{Zr} per h per bar) of Cp_2Zr@Gly, Cp_2Zr@ZrGp and Cp_2Zr@EXZrGP for different times at 60 °C in ethylene polymerization (the system pressure is 1.0×10^6 Pa)

Polymerization time (h)	Cp_2Zr@Gly	Cp_2Zr@ZrGp	Cp_2Zr@EXZrGP
0.5	3.7×10^5	3.0×10^5	4.4×10^5
1.0	3.8×10^5	3.3×10^5	4.8×10^5
1.5	3.8×10^5	3.2×10^5	4.1×10^5
2.0	3.4×10^5	2.8×10^5	3.8×10^5

temperature. The time dependence of the catalytic activity of the catalysts in ethylene polymerization at 60 °C was studied, and 1.0 h was found to be an appropriate time for the catalysts to reach their maximum activities.

The polydispersities (M_w/M_n) and molecular weights of the polyethylene produced in the presence of the catalysts are listed in Table 2. It is found that the M_w/M_n values of the polymers produced by Cp_2Zr@ZrGp and Cp_2Zr@EXZrGP are 2.33 and 2.29, respectively, showing the high dispersity of the active center. The molecular weights of the polymers formed with the catalysts Cp_2Zr@ZrGp and Cp_2Zr@EXZrGP are higher than that of the polymer formed with Cp_2Zr@Gly. Compared to that of Cp_2ZrCl_2@SiO_2, the M_w/M_n values of polymers formed with the catalysts Cp_2Zr@ZrGp and Cp_2Zr@EXZrGP are small and variation ranges are also narrow.

4. Conclusions

Three kinds of new composite metallocene catalyst were synthesized, and their structure and catalytic activity in ethylene polymerization were studied. Results indicate that the content of $ZrCp_2$ increases with an increase in the extent of exposure of amino and carbonyl groups in ZrGP, Gly and exfoliated ZrGP, and the activities of the catalysts in ethylene polymerization increase by the same rule. Due to the connections of $ZrCp_2$ to the hosts by coordination bonds, the risk of exfoliation of the activity center from the support was avoided and the activities of the three synthesized catalysts in ethylene polymerization were all found to be higher than that of Cp_2ZrCl_2@SiO_2, a type of support catalyst now applied in industry. The activities of the three new catalysts are also higher than that of Cp_2ZrCl_2 under the same conditions.

Conflicts of interest

The authors declare no competing financial interest.

Acknowledgements

We thank the projects of the National Natural Science Foundation of China (No. U1362113 and No. 21521005) and the PetroChina Co. Ltd. for financial support.

References

1 K. Kageyama, J. I. Tamazawa and T. Aida, *Science*, 1999, **285**, 2113–2115.
2 J. R. Severn and J. C. Chadwick, *Tailor-made Polymers via Immobilization of Alpha-Olefin Polymerization Catalysts*, Wiley-VCH Verlag GmbH, Weinheim, 2008.
3 G. Natta, P. Pino, G. Mazzanti and U. Giannini, *J. Am. Chem. Soc.*, 1957, **79**, 2975–2976.
4 D. S. Breslow and N. R. Newburg, *J. Am. Chem. Soc.*, 1957, **79**, 5072–5073.
5 S. H. Sinn, W. Kaminsky, H. J. Vollmer and D. C. R. Woldt, *Angew. Chem., Int. Ed. Engl.*, 1980, **19**, 390–392.
6 M. Klapper, J. Daejune, S. Nietzel, J. W. Krumpfer and K. Mullen, *Chem. Mater.*, 2014, **26**, 802–819.
7 R. Huang, R. Duchateau, C. E. Koning and J. C. Chadwick, *Macromolecules*, 2008, **41**, 579–590.
8 D. J. Arriola, E. M. Carnahan, P. D. Hustad, R. L. Kuhlman and T. T. Wenzel, *Science*, 2006, **312**, 714–719.
9 W. Han, C. Muller, D. Vogt, J. W. Niemantsverdriet and P. C. Thune, *Macromol. Rapid Commun.*, 2006, **27**, 279–283.
10 G. G. Hlatky, *Chem. Rev.*, 2000, **100**, 1347–1376.
11 G. J. P. Britovsek, V. C. Gibson, B. S. Kimberley, P. J. Maddox, S. J. McTavish, G. A. Solan, A. J. P. White and D. J. Williams, *Chem. Commun.*, 1998, 849–850.
12 H. G. Alt and A. Koppl, *Chem. Rev.*, 2000, **100**, 1205–1222.
13 J. C. Buffet, N. Wanna, T. A. Q. Arnold, E. K. Gibson, P. P. Wells, Q. Wang, J. Tantirungrotechai and D. O'Hare, *Chem. Mater.*, 2015, **27**, 1495–1501.
14 G. W. Coates, *Chem. Rev.*, 2000, **100**, 1223–1252.
15 G. Albert, U. Costantino, A. Allulli and N. Tomassini, *J. Inorg. Nucl. Chem.*, 1978, **40**, 1113–1117.
16 R. Christian, M. M. Samanamu, J. L. M. Olmstead and F. R. Anne, *Inorg. Chem.*, 2008, **47**(9), 3879–3887.
17 M. V. Vasylyev, E. J. Wachtel, R. Popovitz-Biro and R. Neumann, *Chem.–Eur. J.*, 2006, **12**(13), 3507–3514.
18 Q. H. Xu, Y. Q. Zhang, J. J. Yi, Y. Yuan and S. Mansur, *Microporous Mesoporous Mater.*, 2009, **119**, 68–74.
19 Y. Q. Zhang, M. L. Li, X. M. Ji and Q. H. Xu, *Solid State Sci.*, 2010, **12**, 361–366.
20 Y. J. Jia, Y. J. Zhang, R. W. Wang, F. Y. Fan and Q. H. Xu, *Appl. Surf. Sci.*, 2012, **258**, 2551–2561.
21 B. L. Zhang, D. M. Poojary, A. Clearfield and G. Z. Peng, *Chem. Mater.*, 1996, **8**(6), 1333–1340.
22 L. Britcher, H. Rahiala, K. Hakala, P. Mikkola and J. B. Rosenholm, *Chem. Mater.*, 2004, **16**, 5713–5720.
23 S. G. Feng and R. R. Gordon, *Organometallics*, 2002, **21**, 832–839.
24 S. G. Chen, J. Wang and H. Wang, *Mater. Des.*, 2016, **90**, 84–90.
25 L. Deborah, A. C. Greene and M. Marisa, *J. Organomet. Chem.*, 2003, **682**, 8–13.
26 B. B. Pan, J. J. Ma, X. B. Zhang, L. Liu, D. G. Zhang, J. P. Li, M. Yang, Z. Y. Zhang and Z. W. Tong, *Microporous Mesoporous Mater.*, 2016, **223**(15), 213–218.